

# Primordial black holes and scalar induced secondary gravitational waves from Higgs inflation with noncanonical kinetic term

Jiong Lin,<sup>1,\*</sup> Shengqing Gao,<sup>1,†</sup> Yungui Gong,<sup>1,‡</sup>  
Yizhou Lu,<sup>1,§</sup> Zhongkai Wang,<sup>1,¶</sup> and Fengge Zhang<sup>2,\*\*</sup>

<sup>1</sup>*School of Physics, Huazhong University of Science  
and Technology, Wuhan, Hubei 430074, China*

<sup>2</sup>*School of Physics and Astronomy,  
Sun Yat-sen University, Zhuhai 519088, China*

## Abstract

By combining the noncanonical kinetic term with the nonminimal coupling between gravity and Higgs field, we propose a novel inflationary mechanism and show that the curvature perturbation at small scales can be enhanced by the fluctuations of the Higgs field while satisfying the cosmic microwave background observations at large scales. We find that the recent NANOGrav signal and the black holes in LIGO-Virgo events may originate from the vacuum fluctuations of Higgs field. The cosmological probe of Higgs field by space-based gravitational wave observatory in the future is proposed. We also consider the non-Gaussianity effect on the abundance of primordial black holes and scalar induced secondary gravitational waves. We find that primordial non-Gaussianity makes primordial black holes form more easily, but its effect on the energy density of scalar induced gravitational waves is negligible.

---

\* [jjonglin@hust.edu.cn](mailto:jjonglin@hust.edu.cn)

† [gaoshengqing@hust.edu.cn](mailto:gaoshengqing@hust.edu.cn)

‡ [yggong@hust.edu.cn](mailto:yggong@hust.edu.cn)

§ [louischou@hust.edu.cn](mailto:louischou@hust.edu.cn)

¶ [D202080112@hust.edu.cn](mailto:D202080112@hust.edu.cn)

\*\* Corresponding author. [zhangfg5@mail.sysu.edu.cn](mailto:zhangfg5@mail.sysu.edu.cn)

## I. INTRODUCTION

The overdense inhomogeneities in the radiation era could gravitationally collapse to form primordial black holes (PBHs) [1, 2], which could be used to account for Dark Matters (DM) [3–11]. Due to the vast range of masses, PBHs may explain the Black Hole binaries with tiny effective spin detected by LIGO-Virgo Collaboration [12–15]. These density inhomogeneities can be generated from the inflationary stage, and cause collapse to form PBHs after horizon reentry. This mechanism requires the amplitude of the primordial curvature perturbation to be  $A_s \sim \mathcal{O}(10^{-2})$  [16] while the amplitude has been constrained by the cosmic microwave background (CMB) anisotropy measurements to be  $A_s \approx 2.1 \times 10^{-9}$  at the pivot scale  $k_* = 0.05 \text{ Mpc}^{-1}$  [17]. Thus the enhancement of the amplitude can occur exclusively at small scales.

A way to enhance the curvature perturbation is to provide a dramatic decrease in the velocity of the inflaton, and thus the slow-roll condition is violated. This can be achieved by an inflationary potential with an inflection point [18–20] or a step-like feature [21]. While the inflection point does lead to the decrease in  $\dot{\phi}$ , and thus the enhancement of the power spectrum, it is a challenge to fine-tune the model parameters to enhance the power spectrum to the order of  $\mathcal{O}(10^{-2})$  with the total number of e-folds within  $N \simeq 50 - 60$  [22, 23]. Meanwhile, a new mechanism with a peak function  $G(\phi)$  in the noncanonical kinetic term was proposed to enhance the primordial power spectrum at small scales [24–31]. As we will show in this paper, the peak function serves not only the enhancement of the curvature perturbation, but also the fast exit of inflation keeping the  $e$ -folds around 60. Both sharp and broad peak functions are acceptable [26], which contribute up to  $\sim 20$   $e$ -folds so that the usual slow-roll inflation epoch should be kept around 40  $e$ -folds and the inflationary potential may be restricted. To cure this problem, this mechanism was improved by generalizing the noncanonical kinetic term to  $G(\phi) + f(\phi)$  [25–28]. In this paper, by employing the nonminimal coupling between gravity and scalar field, we will show another way to avoid this potential-restriction problem.

On the other hand, as the only scalar field verified so far, Higgs, if drives inflation, suffers from the problem of unacceptably large tensor-to-scalar ratio  $r$ . To satisfy CMB observation, nonminimal (derivative) couplings  $\xi\phi^2 R$ ,  $G^{\mu\nu}\partial_\mu\phi\partial_\nu\phi$  are introduced to reduce  $r$  [32–39]. Taking into account the running of self-coupling constant and the nonminimal coupling be-

tween Higgs field and gravity, the effective potential in Einstein frame possesses an inflection point, which can enhance the curvature perturbation. However, such an enhancement is only of five orders of magnitude compared with CMB constraint  $A_s \sim O(10^{-9})$ , and is unable to produce a significant abundance of PBHs [40, 41]. In our paper, we will show that, by introducing a noncanonical kinetic term and a nonminimal coupling, the Higgs-field-driving inflation is compatible with CMB observation while simultaneously enhancing the curvature perturbations to order  $\mathcal{O}(10^{-2})$  at small scales.

The production of PBHs by the enhanced primordial curvature perturbation is accompanied by the generation of scalar induced gravitational waves (SIGWs) [42–55], which consist of the stochastic background and can be tested by Pulsar Timing Arrays (PTA) [56–59] and the space based GW observatories like Laser Interferometer Space Antenna (LISA) [60], Taiji [61] and TianQin [62]. Therefore, the observations of both PBHs and SIGWs can be used to constrain the amplitude enhancement of the primordial curvature perturbation during inflation and thus to probe the physics in the early universe.

The paper is organized as follows. In Sec. II, we show our mechanism to enhance the curvature perturbation with Higgs potential by combining the noncanonical kinetic term with the nonminimal coupling. The PBH abundance and the energy density of SIGWs generated by Higgs inflation are presented in Sec. III. In Sec. IV, we discuss the effect of the non-Gaussianity on PBH abundance and SIGWs. We conclude the paper in Sec. V.

## II. THE ENHANCEMENT MECHANISM

An idea to enhance curvature perturbation is to transiently change the friction term in curvature perturbation equation

$$\zeta_k'' + 2\frac{z'}{z}\zeta_k' + k^2\zeta_k = 0, \quad (1)$$

into a driving term during inflation. To wit,  $z'/z < 0$ . For inflation with the noncanonical kinetic term  $(1 + G(\phi))X$  where  $X = \dot{\phi}^2/2$ ,

$$\frac{z'}{z} = aH \left[ 1 + \epsilon_1 - \epsilon_2 + \frac{G_\phi \dot{\phi}}{2H(1 + G)} \right], \quad (2)$$

where  $\epsilon_1 = -\dot{H}/H^2$ ,  $\epsilon_2 = -\ddot{\phi}/(H\dot{\phi})$  are slow-roll parameters. To make  $z'/z < 0$ , we could transiently keep the second slow-roll parameter  $\epsilon_2 > 0$  and large, i.e. the velocity of scalar

field should dramatically decrease. The scalar field equation is

$$H\dot{\phi}(3 - \epsilon_2) + V_\phi^{\text{eff}} = 0, \quad (3)$$

where  $V_\phi^{\text{eff}} = (V_\phi + XG_\phi)/(1 + G)$  and the subscript  $\phi$  represents the derivative with respect to  $\phi$ . As shown in Fig.1, if  $G$  has a peak, then as  $\phi$  rolls down to the red region where  $G_\phi$  is negative and large, the gradient of effective potential satisfies  $V_\phi^{\text{eff}} < 0$  and  $|V_\phi^{\text{eff}}| \gg 1$  so that  $\epsilon_2 \gg 3$  and  $\dot{\phi}$  will dramatically decrease, and thus enhance curvature perturbation. As  $\phi$  leaves for the green region where  $G_\phi$  is positive and very large, the gradient of effective potential  $V_\phi^{\text{eff}} > 0$  and  $|V_\phi^{\text{eff}}| \gg 1$  such that  $\epsilon_2 < 0$  and  $|\epsilon_2| \gg 1$ . Here  $\dot{\phi}$  will violently increase and exit the inflation within several  $e$ -folds.

In a word, phenomenologically, the peak function  $G$  enables not only the dramatic decrease in  $\dot{\phi}$ , which further leads to the enhancement of the curvature perturbation but also the fast exit of inflation with the  $e$ -folds around 60. In fact, by performing a field-redefinition  $d\varphi = \sqrt{1 + G}d\phi$ , our model is equivalent to a class of the canonical inflation with the potential possessing an inflection point [30], as shown in Fig.2.

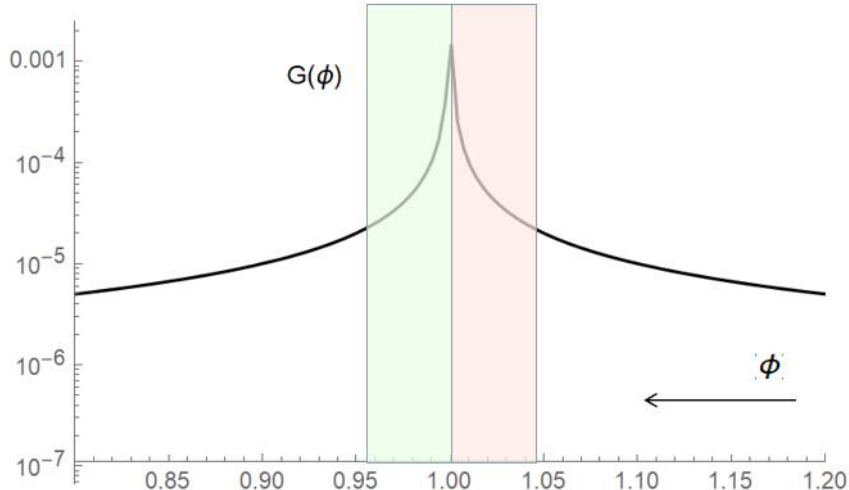


FIG. 1. The red region of the peak function helps the dramatic decrease in  $\dot{\phi}$  and thus the enhancement of the curvature perturbation while the green region of the peak function helps the increase in  $\dot{\phi}$  and thus the exit of inflation with the  $e$ -folds around 60.

On the other hand, under slow-roll approximation, the power spectrum of curvature perturbation takes the form  $\mathcal{P}_\zeta \propto 1 + G$ , which indicates that the curvature perturbation

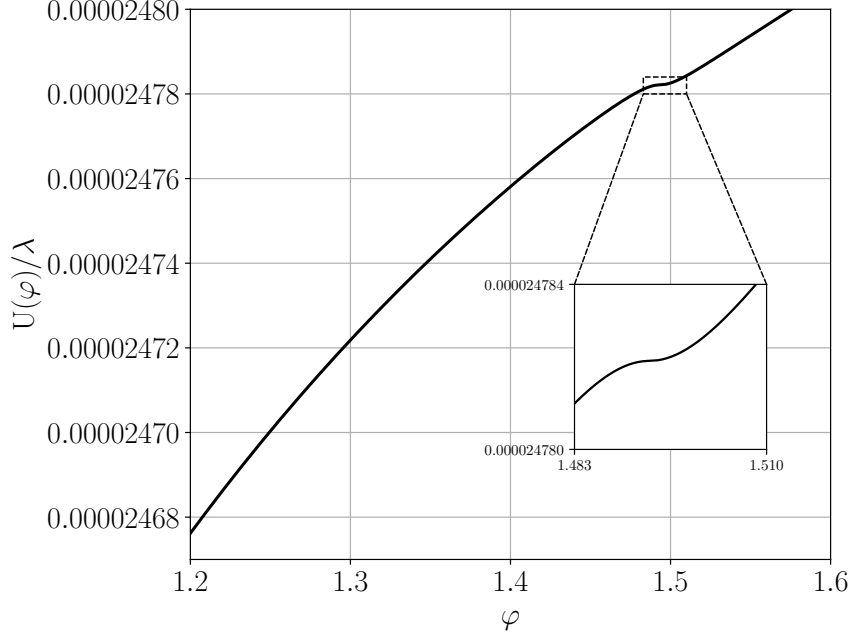


FIG. 2. After the field redefinition, the corresponding canonical potential possesses an inflection point.

can be enhanced with a peaked  $G(\phi)$ . Motivated by Brans-Dicke theory [63] with coupling  $1/\phi^q$ , we choose

$$G(\phi) = \frac{h}{1 + (|\phi - \phi_c|/c)^q}, \quad (4)$$

where  $h, c$  determine the amplitude and width of the peak, respectively.  $q$  controls the shape of the enhanced power spectrum. Larger  $q$  may give a broad peak in the power spectrum. The peak position  $\phi_c$  is related to the peak mass of PBH and the peak frequency of SIGW. Away from the peak,  $G \approx 0$  such that the usual slow-roll inflation is recovered. Note that due to the dramatic decrease in  $\dot{\phi}$ , the peak function  $G(\phi)$  will contribute up to  $\sim 20$   $e$ -folds, and the usual slow-roll inflation epoch should be kept around 40  $e$ -folds so that the total  $e$ -folds during inflation is around 60. For power-law potential  $V = \lambda\phi^p$  with  $0 < p \leq 4$ , the  $e$ -folds during slow-roll inflation can be expressed in terms of the spectrum index as  $N_{sr} \approx (p+2)/2(1-n_s)$ . To keep  $N_{sr} \sim 40$ ,  $p$  should be bounded by  $p \lesssim 1$ . Thus this mechanism does not work for Higgs field ( $p = 4$ ). Besides, the tensor-to-scalar ratio predicted by inflation with Higgs potential is

$$r \approx 8 \left( \frac{V_\phi}{V} \right)^2 = \frac{8p(1-n_s)}{p+2} \Big|_{p=4} \approx 0.18, \quad (5)$$

which is incompatible with observational constraints  $r_{0.05} < 0.036(95\%CL)$  [64].

To realize the enhanced power spectrum with Higgs field, we combine this enhancement mechanism with the nonminimal coupling between Higgs field and gravity, i.e.  $\Omega(\phi)\tilde{R}$ . The action in Jordan frame is

$$S = \int d^4x \sqrt{-\tilde{g}} \left[ \frac{1}{2} \Omega(\phi) \tilde{R}(\tilde{g}) - \frac{1}{2} \omega(\phi) \tilde{g}^{\mu\nu} \nabla_\mu \phi \nabla_\nu \phi - \lambda \phi^p \right]. \quad (6)$$

Under conformal transformation  $g_{\mu\nu} = \Omega(\phi) \tilde{g}_{\mu\nu}$ , the action in Einstein frame becomes

$$S = \int d^4x \sqrt{-g} \left[ \frac{1}{2} R(g) - \frac{1}{2} W(\phi) g^{\mu\nu} \nabla_\mu \phi \nabla_\nu \phi - U(\phi) \right], \quad (7)$$

where

$$W(\phi) = \frac{3}{2} \frac{(d\Omega/d\phi)^2}{\Omega^2(\phi)} + \frac{\omega(\phi)}{\Omega(\phi)}, \quad U(\phi) = \lambda \phi^p / \Omega^2(\phi). \quad (8)$$

To keep the  $e$ -folds of usual slow-roll inflation  $N_{sr} \sim 40$ , we choose the conformal factor

$$\Omega(\phi) = 1 + \xi \phi^{p/2} \quad (9)$$

such that the effective power law of  $U(\phi)$  is  $\lesssim 1$ . The conformal factor flattens the Higgs potential so that the tensor-to-scalar ratio is within the CMB observation. By choosing the appropriate coupling function  $\omega(\phi)$  in Jordan frame, the coupling function in Einstein frame becomes

$$W(\phi) = 1 + G(\phi). \quad (10)$$

TABLE I. The chosen parameters and the results for the scalar power spectrum at small peak scales.

Models	$\phi_*$	$\phi_c$	$\lambda$	$h$	$c$	$N$	$n_s$	$r$	$k_{\text{peak}}/\text{Mpc}^{-1}$	$\mathcal{P}_{\zeta(\text{peak})}$
H1	1.6	1.515	$2.3 \times 10^{-7}$	$8 \times 10^7$	$8.3 \times 10^{-11}$	63	0.97	0.0007	$2.84 \times 10^5$	0.036
H2	1.6	1.3	$2.3 \times 10^{-7}$	$8.15 \times 10^7$	$1.309 \times 10^{-10}$	63	0.966	0.0007	$4 \times 10^{12}$	0.0258
WH	1.6	1.47	$2.3 \times 10^{-7}$	$8 \times 10^7$	$7.445 \times 10^{-10}$	64	0.965	0.0007	$2.99 \times 10^5$	0.016

We use labels "H" and "WH" to represent Higgs inflations with the shape parameter  $q = 1$  and  $q = 6/5$ , respectively. The self-coupling constant  $\lambda$  is set as  $\mathcal{O}(10^{-7})$  to satisfy the amplitude of power spectrum  $A_s \simeq 2 \times 10^{-9}$  at CMB scale. To get  $\mathcal{O}(10^{-2})$  enhancement at small scale, we choose  $h \sim \mathcal{O}(10^7)$ . The nonminimal coupling constant is taken as  $\xi = 100$ . With the model parameters listed in Table I, solving the equations for the background

and the perturbations numerically, the results for the scalar power spectrum are shown in Table I. From these results, we can see that  $n_s$  and  $r$  are well within the CMB observation constraints,  $n_s = 0.9649 \pm 0.0042(68\%CL)$  and  $r_{0.05} < 0.036(95\%CL)$  [17, 64]. In particular, due to conformal factor,  $r$  can be reduced to order  $\mathcal{O}(10^{-4})$ . The total  $e$ -folds are around 60. In Fig. 3, we show the results for the scalar power spectrum. The power spectrum is enhanced to  $\mathcal{O}(10^{-2})$  at the scales  $\mathcal{O}(10^5)\text{Mpc}^{-1}$ ,  $\mathcal{O}(10^{12})\text{Mpc}^{-1}$ . The shape parameter  $q = 1$  produces a sharp peak while the larger shape parameter  $q = 6/5$  produces the broad peak. The models also satisfy the constraints from CMB  $\mu$ -distortion, big bang nucleosynthesis (BBN) and pulsar timing array (PTA) observations [65–67].

One may wonder about the effect of the running of self-coupling constant. In fact, by expanding the self-coupling constant around the inflation scale  $\mu$  as  $\lambda(\phi) = \lambda + \lambda_1 \ln^2(\phi/\mu)$  and choosing  $\lambda \gg \lambda_1$  to avoid the emergence of the inflection point in the potential, the result for the enhanced power spectrum is almost invariant up to  $\mathcal{O}(\lambda_1/\lambda)$  order correction.

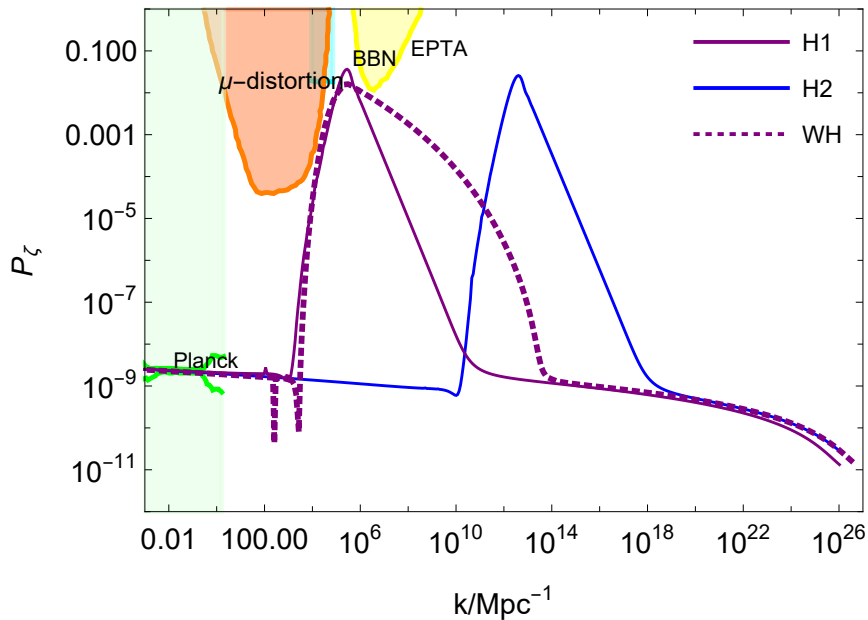


FIG. 3. The results for the scalar power spectrum for Model H1 (the purple line), Model H2 (the blue line) and model WH (the dotted purple line). The green lines show the scale-dependent behavior of the power spectrum. The lightgreen shaded region is excluded by the CMB observations [17]. The orange, cyan and yellow regions show the constraints from  $\mu$ -distortion of CMB [67], the effect on the ratio between neutron and proton during the big bang nucleosynthesis (BBN) [66] and the PTA observations [65], respectively.

### III. PBH AND SIGW

The overdense region would gravitationally collapse to form PBHs when horizon reentry during radiation dominated era. The current fractional energy density of PBHs with mass  $M$  to DM is [8, 20]

$$Y_{\text{PBH}}(M) = \frac{\beta(M)}{3.94 \times 10^{-9}} \left(\frac{\gamma}{0.2}\right)^{1/2} \left(\frac{g_*}{10.75}\right)^{-1/4} \left(\frac{0.12}{\Omega_{\text{DM}} h^2}\right) \left(\frac{M}{M_\odot}\right)^{-1/2}, \quad (11)$$

where  $M_\odot$  is the solar mass,  $\gamma = 0.2$  [68].  $g_*$  is the effective degrees of freedom at the formation time. For the temperature  $T > 300$  GeV,  $g_* = 107.5$  and for  $0.5$  MeV  $< T < 300$  GeV,  $g_* = 10.75$ .  $\Omega_{\text{DM}}$  is the current energy density parameter of DM and we take  $\Omega_{\text{DM}} h^2 = 0.12$  [69]. The PBH mass  $M$  is related to the scale  $k$  as [20]

$$M(k) = 3.68 \left(\frac{\gamma}{0.2}\right) \left(\frac{g_*}{10.75}\right)^{-1/6} \left(\frac{k}{10^6 \text{ Mpc}^{-1}}\right)^{-2} M_\odot. \quad (12)$$

$\beta(M)$  is the fractional energy density of PBHs at the formation. For Gaussian comoving curvature perturbation  $\zeta$  [70, 71], we have

$$\beta^G(M) \approx \sqrt{\frac{2}{\pi}} \frac{\sqrt{\mathcal{P}_\zeta}}{\mu_c} \exp\left(-\frac{\mu_c^2}{2\mathcal{P}_\zeta}\right), \quad (13)$$

where  $\delta_c$  is the threshold for the PBH formation and  $\mu_c = 9\sqrt{2}\delta_c/4$  [26]. Here we choose  $\delta_c = 0.4$  [71–75] for calculations.

Accompanied by the production of PBHs, the large curvature perturbation from inflation can induce GWs at radiation era. The Fourier components of the second order tensor perturbations  $h_{\mathbf{k}}$  satisfy [44, 45]

$$h''_{\mathbf{k}} + 2\mathcal{H}h'_{\mathbf{k}} + k^2 h_{\mathbf{k}} = 4S_{\mathbf{k}}, \quad (14)$$

with the source of scalar perturbations

$$S_{\mathbf{k}} = \int \frac{d^3 \tilde{\mathbf{k}}}{(2\pi)^{3/2}} e_{ij}(\mathbf{k}) \tilde{k}^i \tilde{k}^j \left[ 2\Phi_{\tilde{\mathbf{k}}} \Phi_{\mathbf{k}-\tilde{\mathbf{k}}} + \frac{4}{3(1+\omega)\mathcal{H}^2} \times (\Phi'_{\tilde{\mathbf{k}}} + \mathcal{H}\Phi_{\tilde{\mathbf{k}}}) (\Phi'_{\mathbf{k}-\tilde{\mathbf{k}}} + \mathcal{H}\Phi_{\mathbf{k}-\tilde{\mathbf{k}}}) \right], \quad (15)$$

where  $\mathcal{H} = aH$ ,  $\omega = p/\rho$ ,  $e_{ij}(\mathbf{k})$  is the polarization tensor. The Bardeen potential

$$\Phi_{\mathbf{k}} = \Psi(k\eta)\phi_{\mathbf{k}}, \quad (16)$$

where the transfer function  $\Psi$  in the radiation domination is

$$\Psi(x) = \frac{9}{x^2} \left( \frac{\sin(x/\sqrt{3})}{x/\sqrt{3}} - \cos(x/\sqrt{3}) \right), \quad (17)$$

and the primordial value  $\phi_{\mathbf{k}}$  is

$$\langle \phi_{\mathbf{k}} \phi_{\tilde{\mathbf{k}}} \rangle = \delta^{(3)}(\mathbf{k} + \tilde{\mathbf{k}}) \frac{2\pi^2}{k^3} \left( \frac{3 + 3w}{5 + 3w} \right)^2 \mathcal{P}_\zeta(k). \quad (18)$$

The power spectrum of the induced GWs is defined as

$$\langle h_{\mathbf{k}}(\eta) h_{\tilde{\mathbf{k}}}(\eta) \rangle = \frac{2\pi^2}{k^3} \delta^{(3)}(\mathbf{k} + \tilde{\mathbf{k}}) \mathcal{P}_h(k, \eta). \quad (19)$$

The current energy densities of GWs are

$$\Omega_{GW}(k, \eta_0) = \frac{1}{24} \frac{\Omega_r(\eta_0)}{\Omega_r(\eta)} \left( \frac{k}{aH} \right)^2 \overline{\mathcal{P}_h(k, \eta)}, \quad (20)$$

where  $\Omega_r$  is the fraction energy density of radiation and  $\overline{\mathcal{P}_h(k, \eta)}$  is the oscillation time average. Combining Eqs.(14),(18) and (19), the current energy densities of GWs can be expressed in terms of the primordial scalar perturbation power spectrum as

$$\begin{aligned} \Omega_{GW}(k, \eta_0) = & \frac{1}{6} \frac{\Omega_r(\eta_0)}{\Omega_r(\eta)} \left( \frac{k}{aH} \right)^2 \int_0^\infty dv \int_{|1-v|}^{1+v} du \left\{ \left[ \frac{4v^2 - (1 - u^2 + v^2)^2}{4uv} \right]^2 \right. \\ & \left. \times \overline{I_{RD}^2(u, v, x \rightarrow \infty)} \mathcal{P}_\zeta(kv) \mathcal{P}_\zeta(ku) \right\}, \end{aligned} \quad (21)$$

where  $u = |\mathbf{k} - \tilde{\mathbf{k}}|/k$ ,  $v = \tilde{k}/k$ ,  $x = k\eta$  and

$$\begin{aligned} I_{RD} = & \int_1^x dy y \sin(x - y) \{ 3\Psi(uy)\Psi(vy) \\ & + y[\Psi(vy)u\Psi'(uy) + v\Psi'(vy)\Psi(uy)] + y^2 uv\Psi'(uy)\Psi'(vy) \} \end{aligned} \quad (22)$$

is the integral kernel. The analytical expression for  $I_{RD}$  was given in Refs. [76, 77].

Substituting the obtained power spectrum into Eqs.(11) and (21), we get the PBH abundances <sup>1</sup> as shown in Table.II and Fig.4 and the current energy densities of SIGWs as shown in Fig.5. Mdoel H1 produces PBHs with mass  $M \simeq 30M_\odot$  and the abundance  $Y^{\text{peak}} \simeq 5.3 \times 10^{-4}$ , which may explain the BH event GW150914 observed by LIGO [12]. The accompanying SIGWs have the peak frequency  $f \sim 4.8 \times 10^{-10}\text{Hz}$  and could be tested

---

<sup>1</sup> Here we use the Gaussian formulate Eq.(13) for the fraction energy density of PBHs at the formation.

Next section the non-Gaussianity effect will be taken into account.

by SKA. Although Model WH can not produce significant PBHs using the Gaussian formulate Eq.(13) , the energy density of SIGWs lies within the  $2\sigma$  region of the NANOGrav signal [78–84]. Thus NANOGrav signal and the BHs in LIGO-Virgo events may both originate from the Higgs field. Models H2 produces PBHs with mass  $M \simeq \mathcal{O}(10^{-13})M_\odot$ . In these mass ranges, PBHs can constitute almost all DM. The accompanying SIGWs has the millihertz frequency, which can be tested by future space-based detectors like LISA, TaiJi, and TianQin.

TABLE II. The results for PBH abundance and critical frequency of SIGWs.

Model	$k_{\text{peak}}/\text{Mpc}^{-1}$	$\mathcal{P}_\zeta(\text{peak})$	$M_{\text{pbh}}^{\text{peak}}/M_\odot$	$Y_{\text{PBH}(\text{peak})}^G$	$f_c/\text{Hz}$
H1	$2.84 \times 10^5$	0.036	29	$5.3 \times 10^{-4}$	$4.8 \times 10^{-10}$
H2	$4 \times 10^{12}$	0.0258	$1.48 \times 10^{-13}$	0.88	$6.8 \times 10^{-3}$
WH	$2.99 \times 10^5$	0.016			$5 \times 10^{-10}$

#### IV. NON-GAUSSIANITY

Due to the violation of the slow-roll condition, the non-Gaussianity may be large. Thus it is necessary to investigate the impact of non-Gaussianity on PBH abundance and SIGWs. The non-Gaussianity parameter  $f_{\text{NL}}$  is [94]

$$f_{\text{NL}}(k_1, k_2, k_3) = \frac{5}{6} \frac{B_\zeta(k_1, k_2, k_3)}{P_\zeta(k_1)P_\zeta(k_2) + P_\zeta(k_2)P_\zeta(k_3) + P_\zeta(k_3)P_\zeta(k_1)}, \quad (23)$$

where  $P_\zeta(k) = 2\pi^2 \mathcal{P}_\zeta(k)/k^3$  and the bispectrum is defined as

$$\langle \hat{\zeta}_{\mathbf{k}_1} \hat{\zeta}_{\mathbf{k}_2} \hat{\zeta}_{\mathbf{k}_3} \rangle = (2\pi)^3 \delta^3(\mathbf{k}_1 + \mathbf{k}_2 + \mathbf{k}_3) B_\zeta(k_1, k_2, k_3). \quad (24)$$

With the non-Gaussianity correction, the fraction energy density of PBH at the formation becomes [95–98]

$$\beta = e^{\Delta_3} \beta^G. \quad (25)$$

The mass of PBHs we consider is almost monochromatic, thus the third cumulant  $\Delta_3$  can be approximately expressed as [30]

$$\Delta_3 \approx 23 \frac{\delta_c^3}{\mathcal{P}_\zeta(k_{\text{peak}})} f_{\text{NL}}(k_{\text{peak}}, k_{\text{peak}}, k_{\text{peak}}). \quad (26)$$

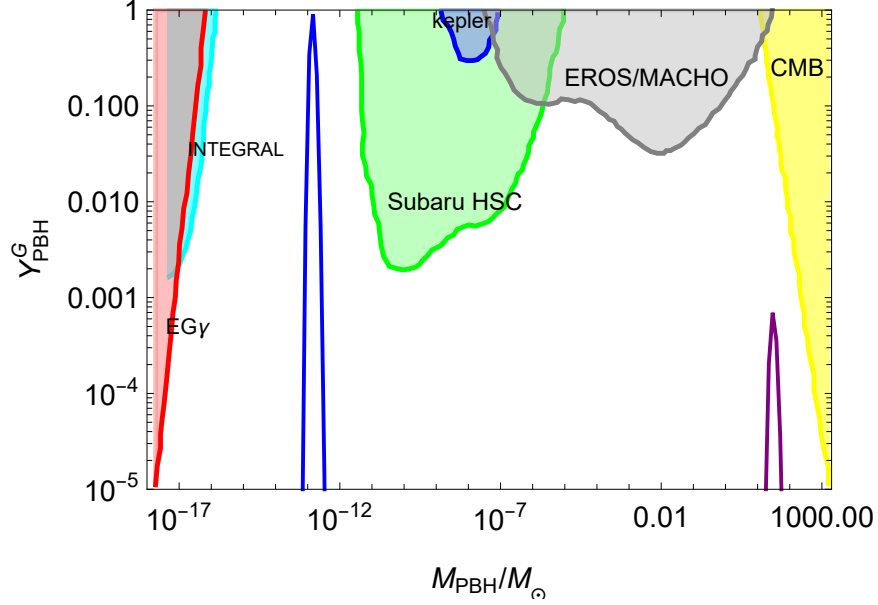


FIG. 4. The PBH abundances for Model H1 (the purple line) and Model H2 (the blue line) using the Gaussian formulate  $\beta^G$  for the fraction energy density of PBHs at the formation. The shaded regions show the observational constraints on the PBH abundance: the red region from extragalactic gamma-rays by PBH evaporation (EG $\gamma$ ) [85], the cyan region from galactic center 511 keV gamma-ray line (INTEGRAL) [86, 87], the green region from microlensing events with Subaru HSC [88], the blue region from the Kepler satellite [89], the gray region from the EROS/MACHO [90] and the yellow region from accretion constraints by CMB [91, 92].

In Table.III, we show the results for the non-Gaussianity parameter  $f_{\text{NL}}$  and the third cumulant  $\Delta_3$ . The non-Gaussianity parameter  $f_{\text{NL}}$  is of order  $\mathcal{O}(10^{-1})$ . In fact, during inflation with the sharper peak, the second slow-roll parameter  $\epsilon_2$  changes more dramatically such that the non-Gaussianity effect is more significant than inflation with the broad peak. The non-Gaussianity correction has a significant enhancement on PBH abundance, which means the formation of PBHs is easier with the consideration of the non-Gaussianity. The PBH abundance is underestimated with Gaussian statistics.

To investigate the non-Gaussian effect on SIGWs, we first consider the power spectrum with the non-Gaussian correction. With the nonlinear corrections, the comoving curvature perturbation can be expressed as [99, 100]

$$\zeta(\mathbf{x}) = \zeta^G(\mathbf{x}) + \frac{3}{5}f_{\text{NL}}(\zeta^G(\mathbf{x})^2 - \langle \zeta^G(\mathbf{x})^2 \rangle), \quad (27)$$

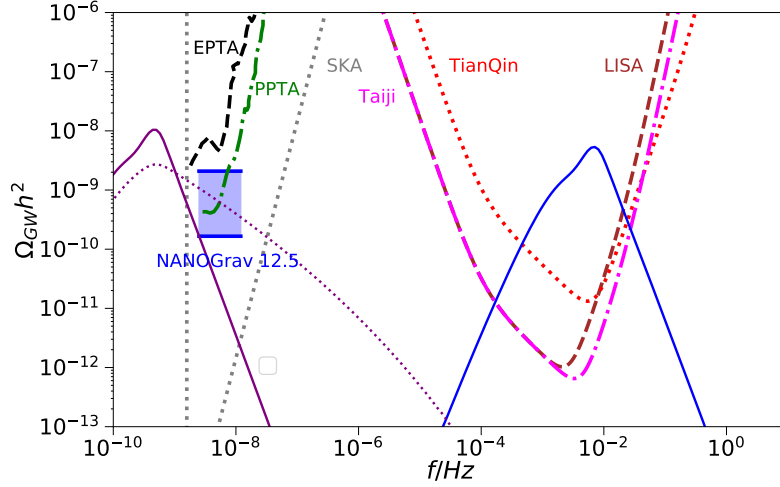


FIG. 5. The SIGWs from Model H1 (the purple line), Model H2 (the blue line) and WH (the dotted purple line). The black dashed curve shows the EPTA limit [56–59], the grey dotted curve denotes the SKA limit [93], the brown dashed curve shows the LISA limit [60], the red dot-dashed curve denotes the TianQin limit [62] and the dotted magenta curve denotes the TaiJi limit [61]

TABLE III. The results for the non-Gaussianity parameter  $f_{\text{NL}}$  and the third cumulant  $\Delta_3$ .

Model	$f_{\text{NL}}(k_{\text{peak}}, k_{\text{peak}}, k_{\text{peak}})$	$\Delta_3$
H1	0.62	25
H2	0.53	30
WH	0.13	12

where  $\zeta^G$  is the Gaussian part of the curvature perturbation. Thus the power spectrum is

$$\mathcal{P}_\zeta(k) = \mathcal{P}_\zeta^G(k) + \mathcal{P}_\zeta^{\text{NG}}(k), \quad (28)$$

with the non-Gaussianity correction of the power spectrum

$$\mathcal{P}_\zeta^{\text{NG}}(k) = \left(\frac{3}{5}\right)^2 \frac{k^3}{2\pi} f_{\text{NL}}^2 \int d^3\mathbf{p} \frac{\mathcal{P}_\zeta^G(p)}{p^3} \frac{\mathcal{P}_\zeta^G(|\mathbf{k} - \mathbf{p}|)}{|\mathbf{k} - \mathbf{p}|^3}. \quad (29)$$

For our model with  $f_{\text{NL}} \sim \mathcal{O}(10^{-1})$  at peak scales, we have  $\mathcal{P}_\zeta^{\text{NG}}(k) \ll \mathcal{P}_\zeta^G(k)$  and thus the non-Gaussianity effect can be neglected when calculating SIGWs.

## V. CONCLUSIONS

Inflation with a noncanonical kinetic term  $(1 + G(\phi))X$  can produce enhanced curvature perturbations at small scales if the coupling function  $G(\phi)$  has a peak. Phenomenologically, the peak function  $G$  not only drives the dramatic decreases in  $\dot{\phi}$  (henceforth provides an effective inflection point) and thus the enhancement of the curvature perturbation but also helps the exit of inflation while keeping  $e$ -folds around 60. Due to the dramatic decrease in  $\dot{\phi}$ , the peak function  $G(\phi)$  will contribute up to  $\sim 20$   $e$ -folds and the usual slow-roll inflation epoch endures around 40  $e$ -folds. For power-law potential  $V = \lambda\phi^p$ , this indicates  $p$  should be bounded as  $p \lesssim 1$ . In particular, this mechanism does not work for Higgs potential  $V = \lambda\phi^4$ . On the other hand, Higgs inflation with nonminimal coupling satisfies the constraints from cosmic microwave background observations. To produce PBHs and SIGWs in Higgs inflation, we introduce the noncanonical kinetic term with a peak function and show that the curvature perturbation at small scales can be enhanced by the Higgs field while satisfying the constraints from cosmic microwave background observations. To be specific, in the Einstein frame, the conformal factor flattens the Higgs potential such that the effective power  $p \lesssim 1$  and thus the  $e$ -folds during slow-roll inflation is within 40 and the tensor-to-scalar ratio is reduced.

By varying the peak position, the curvature perturbation can be enhanced at different scales and thus different mass ranges of PBHs and frequencies of SIGWs can be produced. In particular, PBHs with mass  $\mathcal{O}(10)M_\odot$ ,  $\mathcal{O}(10^{-12})M_\odot$  may explain BHs in LIGO-Virgo events and almost all the DM, respectively. The energy density of SIGWs from the model WH lies within the  $2\sigma$  region of the NANOGrav signal. Thus NANOGrav signal may originate from the Higgs field. SIGWs from the model H2 have the millihertz frequency, which can be tested by future space-based detectors like LISA, TaiJi, and TianQin.

Due to the violation of the slow-roll condition, the non-Gaussianity may have a significant effect on PBH abundance and SIGWs. We find that the non-Gaussianity parameter  $f_{\text{NL}}$  is of order  $\mathcal{O}(10^{-1})$  at peak scales and the non-Gaussianity correction has a significant enhancement on PBH abundance. Notwithstanding, the energy density of SIGWs remains invariant even if we take the non-Gaussianity into account, as the power spectrum receives very tiny corrections.

## ACKNOWLEDGMENTS

This research is supported in part by the National Natural Science Foundation of China under Grant No. 11875136, and the Major Program of the National Natural Science Foundation of China under Grant No. 11690021.

- 
- [1] B. J. Carr and S. W. Hawking, Black holes in the early Universe, *Mon. Not. Roy. Astron. Soc.* **168**, 399 (1974).
  - [2] S. Hawking, Gravitationally collapsed objects of very low mass, *Mon. Not. Roy. Astron. Soc.* **152**, 75 (1971).
  - [3] P. Ivanov, P. Naselsky, and I. Novikov, Inflation and primordial black holes as dark matter, *Phys. Rev. D* **50**, 7173 (1994).
  - [4] P. H. Frampton, M. Kawasaki, F. Takahashi, and T. T. Yanagida, Primordial Black Holes as All Dark Matter, *J. Cosmol. Astropart. Phys.* **04** (2010) 023, [arXiv:1001.2308](#).
  - [5] K. M. Belotsky, A. D. Dmitriev, E. A. Esipova, V. A. Gani, A. V. Grobov, M. Y. Khlopov, A. A. Kirillov, S. G. Rubin, and I. V. Svadkovsky, Signatures of primordial black hole dark matter, *Mod. Phys. Lett. A* **29**, 1440005 (2014), [arXiv:1410.0203](#).
  - [6] M. Y. Khlopov, S. G. Rubin, and A. S. Sakharov, Primordial structure of massive black hole clusters, *Astropart. Phys.* **23**, 265 (2005), [arXiv:astro-ph/0401532](#).
  - [7] S. Clesse and J. García-Bellido, Massive Primordial Black Holes from Hybrid Inflation as Dark Matter and the seeds of Galaxies, *Phys. Rev. D* **92**, 023524 (2015), [arXiv:1501.07565](#).
  - [8] B. Carr, F. Kuhnel, and M. Sandstad, Primordial Black Holes as Dark Matter, *Phys. Rev. D* **94**, 083504 (2016), [arXiv:1607.06077](#).
  - [9] K. Inomata, M. Kawasaki, K. Mukaida, Y. Tada, and T. T. Yanagida, Inflationary Primordial Black Holes as All Dark Matter, *Phys. Rev. D* **96**, 043504 (2017), [arXiv:1701.02544](#).
  - [10] J. García-Bellido, Massive Primordial Black Holes as Dark Matter and their detection with Gravitational Waves, *J. Phys. Conf. Ser.* **840**, 012032 (2017), [arXiv:1702.08275](#).
  - [11] E. D. Kovetz, Probing Primordial-Black-Hole Dark Matter with Gravitational Waves, *Phys. Rev. Lett.* **119**, 131301 (2017), [arXiv:1705.09182](#).
  - [12] B. P. Abbott *et al.* (LIGO Scientific, Virgo), Observation of Gravitational Waves from a

- Binary Black Hole Merger, *Phys. Rev. Lett.* **116**, 061102 (2016), [arXiv:1602.03837](#).
- [13] B. P. Abbott *et al.* (LIGO Scientific, Virgo), GW151226: Observation of Gravitational Waves from a 22-Solar-Mass Binary Black Hole Coalescence, *Phys. Rev. Lett.* **116**, 241103 (2016), [arXiv:1606.04855](#).
- [14] S. Bird, I. Cholis, J. B. Muñoz, Y. Ali-Haïmoud, M. Kamionkowski, E. D. Kovetz, A. Racanelli, and A. G. Riess, Did LIGO detect dark matter?, *Phys. Rev. Lett.* **116**, 201301 (2016), [arXiv:1603.00464](#).
- [15] M. Sasaki, T. Suyama, T. Tanaka, and S. Yokoyama, Primordial Black Hole Scenario for the Gravitational-Wave Event GW150914, *Phys. Rev. Lett.* **117**, 061101 (2016), [Erratum: *Phys.Rev.Lett.* 121, 059901 (2018)], [arXiv:1603.08338](#).
- [16] G. Sato-Polito, E. D. Kovetz, and M. Kamionkowski, Constraints on the primordial curvature power spectrum from primordial black holes, *Phys. Rev. D* **100**, 063521 (2019), [arXiv:1904.10971](#).
- [17] Y. Akrami *et al.* (Planck), Planck 2018 results. X. Constraints on inflation, *Astron. Astrophys.* **641**, A10 (2020), [arXiv:1807.06211](#).
- [18] C. Germani and T. Prokopec, On primordial black holes from an inflection point, *Phys. Dark Univ.* **18**, 6 (2017), [arXiv:1706.04226](#).
- [19] H. Motohashi and W. Hu, Primordial Black Holes and Slow-Roll Violation, *Phys. Rev. D* **96**, 063503 (2017), [arXiv:1706.06784](#).
- [20] H. Di and Y. Gong, Primordial black holes and second order gravitational waves from ultra-slow-roll inflation, *J. Cosmol. Astropart. Phys.* **07** (2018) 007, [arXiv:1707.09578](#).
- [21] K. Inomata, E. McDonough, and W. Hu, Amplification of Primordial Perturbations from the Rise or Fall of the Inflaton, (2021), [arXiv:2110.14641](#).
- [22] M. Sasaki, T. Suyama, T. Tanaka, and S. Yokoyama, Primordial black holes—perspectives in gravitational wave astronomy, *Class. Quant. Grav.* **35**, 063001 (2018), [arXiv:1801.05235](#).
- [23] S. Passaglia, W. Hu, and H. Motohashi, Primordial black holes and local non-Gaussianity in canonical inflation, *Phys. Rev. D* **99**, 043536 (2019), [arXiv:1812.08243](#).
- [24] J. Lin, Q. Gao, Y. Gong, Y. Lu, C. Zhang, and F. Zhang, Primordial black holes and secondary gravitational waves from  $k$  and  $G$  inflation, *Phys. Rev. D* **101**, 103515 (2020), [arXiv:2001.05909](#).
- [25] Z. Yi, Y. Gong, B. Wang, and Z.-h. Zhu, Primordial black holes and secondary gravitational

- waves from the Higgs field, *Phys. Rev. D* **103**, 063535 (2021), [arXiv:2007.09957](#).
- [26] Z. Yi, Q. Gao, Y. Gong, and Z.-h. Zhu, Primordial black holes and scalar-induced secondary gravitational waves from inflationary models with a noncanonical kinetic term, *Phys. Rev. D* **103**, 063534 (2021), [arXiv:2011.10606](#).
- [27] Q. Gao, Y. Gong, and Z. Yi, Primordial black holes and secondary gravitational waves from natural inflation, *Nucl. Phys. B* **969**, 115480 (2021), [arXiv:2012.03856](#).
- [28] Z. Yi and Z.-H. Zhu, NANOGrav signal and LIGO-Virgo Primordial Black Holes from Higgs inflation, (2021), [arXiv:2105.01943](#).
- [29] F. Zhang, Y. Gong, J. Lin, Y. Lu, and Z. Yi, Primordial non-Gaussianity from G-inflation, *J. Cosmol. Astropart. Phys.* **04** (2021) 045, [arXiv:2012.06960](#).
- [30] F. Zhang, J. Lin, and Y. Lu, Double-peaked inflation model: Scalar induced gravitational waves and primordial-black-hole suppression from primordial non-Gaussianity, *Phys. Rev. D* **104**, 063515 (2021), [arXiv:2106.10792](#).
- [31] M. Solbi and K. Karami, Primordial black holes and induced gravitational waves in  $k$ -inflation, *J. Cosmol. Astropart. Phys.* **08** (2021) 056, [arXiv:2102.05651](#).
- [32] D. I. Kaiser, Primordial spectral indices from generalized Einstein theories, *Phys. Rev. D* **52**, 4295 (1995), [arXiv:astro-ph/9408044](#).
- [33] F. L. Bezrukov and M. Shaposhnikov, The Standard Model Higgs boson as the inflaton, *Phys. Lett. B* **659**, 703 (2008), [arXiv:0710.3755](#).
- [34] C. Germani and A. Kehagias, New Model of Inflation with Non-minimal Derivative Coupling of Standard Model Higgs Boson to Gravity, *Phys. Rev. Lett.* **105**, 011302 (2010), [arXiv:1003.2635](#).
- [35] C. Germani, Y. Watanabe, and N. Wintergerst, Self-unitarization of New Higgs Inflation and compatibility with Planck and BICEP2 data, *J. Cosmol. Astropart. Phys.* **12** (2014) 009, [arXiv:1403.5766](#).
- [36] Y. Hamada, H. Kawai, K.-y. Oda, and S. C. Park, Higgs Inflation is Still Alive after the Results from BICEP2, *Phys. Rev. Lett.* **112**, 241301 (2014), [arXiv:1403.5043](#).
- [37] N. Yang, Q. Fei, Q. Gao, and Y. Gong, Inflationary models with non-minimally derivative coupling, *Class. Quant. Grav.* **33**, 205001 (2016), [arXiv:1504.05839](#).
- [38] J. Fumagalli, S. Mooij, and M. Postma, Unitarity and predictiveness in new Higgs inflation, *J. High Energ. Phys.* **03** (2018) 038, [arXiv:1711.08761](#).

- [39] J. Fumagalli, M. Postma, and M. Van Den Bout, Matching and running sensitivity in non-renormalizable in ationary models, *J. High Energ. Phys.* **09** (2020) 114, [arXiv:2005.05905](#).
- [40] J. M. Ezquiaga, J. Garcia-Bellido, and E. Ruiz Morales, Primordial Black Hole production in Critical Higgs Inflation, *Phys. Lett. B* **776**, 345 (2018), [arXiv:1705.04861](#).
- [41] F. Bezrukov, M. Pauly, and J. Rubio, On the robustness of the primordial power spectrum in renormalized Higgs inflation, *J. Cosmol. Astropart. Phys.* **02** (2018) 040, [arXiv:1706.05007](#).
- [42] S. Matarrese, S. Mollerach, and M. Bruni, Second order perturbations of the Einstein-de Sitter universe, *Phys. Rev. D* **58**, 043504 (1998), [arXiv:astro-ph/9707278](#).
- [43] S. Mollerach, D. Harari, and S. Matarrese, CMB polarization from secondary vector and tensor modes, *Phys. Rev. D* **69**, 063002 (2004), [arXiv:astro-ph/0310711](#).
- [44] K. N. Ananda, C. Clarkson, and D. Wands, The Cosmological gravitational wave background from primordial density perturbations, *Phys. Rev. D* **75**, 123518 (2007), [arXiv:gr-qc/0612013](#).
- [45] D. Baumann, P. J. Steinhardt, K. Takahashi, and K. Ichiki, Gravitational Wave Spectrum Induced by Primordial Scalar Perturbations, *Phys. Rev. D* **76**, 084019 (2007), [arXiv:hep-th/0703290](#).
- [46] J. Garcia-Bellido, M. Peloso, and C. Unal, Gravitational Wave signatures of inflationary models from Primordial Black Hole Dark Matter, *J. Cosmol. Astropart. Phys.* **09** (2017) 013, [arXiv:1707.02441](#).
- [47] R. Saito and J. Yokoyama, Gravitational wave background as a probe of the primordial black hole abundance, *Phys. Rev. Lett.* **102**, 161101 (2009), [Erratum: *Phys.Rev.Lett.* 107, 069901 (2011)], [arXiv:0812.4339](#).
- [48] R. Saito and J. Yokoyama, Gravitational-Wave Constraints on the Abundance of Primordial Black Holes, *Prog. Theor. Phys.* **123**, 867 (2010), [Erratum: *Prog.Theor.Phys.* 126, 351–352 (2011)], [arXiv:0912.5317](#).
- [49] E. Bugaev and P. Klimai, Induced gravitational wave background and primordial black holes, *Phys. Rev. D* **81**, 023517 (2010), [arXiv:0908.0664](#).
- [50] E. Bugaev and P. Klimai, Constraints on the induced gravitational wave background from primordial black holes, *Phys. Rev. D* **83**, 083521 (2011), [arXiv:1012.4697](#).
- [51] L. Alabidi, K. Kohri, M. Sasaki, and Y. Sendouda, Observable Spectra of Induced Gravitational Waves from Inflation, *J. Cosmol. Astropart. Phys.* **09** (2012) 017, [arXiv:1203.4663](#).
- [52] N. Orlofsky, A. Pierce, and J. D. Wells, Inflationary theory and pulsar timing investiga-

- tions of primordial black holes and gravitational waves, *Phys. Rev. D* **95**, 063518 (2017), [arXiv:1612.05279](#).
- [53] T. Nakama, J. Silk, and M. Kamionkowski, Stochastic gravitational waves associated with the formation of primordial black holes, *Phys. Rev. D* **95**, 043511 (2017), [arXiv:1612.06264](#).
- [54] K. Inomata, M. Kawasaki, K. Mukaida, Y. Tada, and T. T. Yanagida, Inflationary primordial black holes for the LIGO gravitational wave events and pulsar timing array experiments, *Phys. Rev. D* **95**, 123510 (2017), [arXiv:1611.06130](#).
- [55] S.-L. Cheng, W. Lee, and K.-W. Ng, Primordial black holes and associated gravitational waves in axion monodromy inflation, *J. Cosmol. Astropart. Phys.* **07** (2018) 001, [arXiv:1801.09050](#).
- [56] R. D. Ferdman *et al.*, The European Pulsar Timing Array: current efforts and a LEAP toward the future, *Class. Quant. Grav.* **27**, 084014 (2010), [arXiv:1003.3405](#).
- [57] G. Hobbs *et al.*, The international pulsar timing array project: using pulsars as a gravitational wave detector, *Class. Quant. Grav.* **27**, 084013 (2010), [arXiv:0911.5206](#).
- [58] M. A. McLaughlin, The North American Nanohertz Observatory for Gravitational Waves, *Class. Quant. Grav.* **30**, 224008 (2013), [arXiv:1310.0758](#).
- [59] G. Hobbs, The Parkes Pulsar Timing Array, *Class. Quant. Grav.* **30**, 224007 (2013), [arXiv:1307.2629](#).
- [60] P. Amaro-Seoane *et al.* (LISA), Laser Interferometer Space Antenna, (2017), [arXiv:1702.00786](#).
- [61] W.-R. Hu and Y.-L. Wu, The Taiji Program in Space for gravitational wave physics and the nature of gravity, *Natl. Sci. Rev.* **4**, 685 (2017).
- [62] J. Luo *et al.* (TianQin), TianQin: a space-borne gravitational wave detector, *Class. Quant. Grav.* **33**, 035010 (2016), [arXiv:1512.02076](#).
- [63] C. Brans and R. H. Dicke, Mach's principle and a relativistic theory of gravitation, *Phys. Rev.* **124**, 925 (1961).
- [64] P. A. R. Ade *et al.* (BICEP, Keck), Improved Constraints on Primordial Gravitational Waves using Planck, WMAP, and BICEP/Keck Observations through the 2018 Observing Season, *Phys. Rev. Lett.* **127**, 151301 (2021), [arXiv:2110.00483](#).
- [65] K. Inomata and T. Nakama, Gravitational waves induced by scalar perturbations as probes of the small-scale primordial spectrum, *Phys. Rev. D* **99**, 043511 (2019), [arXiv:1812.00674](#).

- [66] K. Inomata, M. Kawasaki, and Y. Tada, Revisiting constraints on small scale perturbations from big-bang nucleosynthesis, *Phys. Rev. D* **94**, 043527 (2016), [arXiv:1605.04646](#).
- [67] D. J. Fixsen, E. S. Cheng, J. M. Gales, J. C. Mather, R. A. Shafer, and E. L. Wright, The Cosmic Microwave Background spectrum from the full COBE FIRAS data set, *Astrophys. J.* **473**, 576 (1996), [arXiv:astro-ph/9605054](#).
- [68] B. J. Carr, The Primordial black hole mass spectrum, *Astrophys. J.* **201**, 1 (1975).
- [69] N. Aghanim *et al.* (Planck), Planck 2018 results. VI. Cosmological parameters, *Astron. Astrophys.* **641**, A6 (2020), [Erratum: *Astron. Astrophys.* 652, C4 (2021)], [arXiv:1807.06209](#).
- [70] O. Özsoy, S. Parameswaran, G. Tasinato, and I. Zavala, Mechanisms for Primordial Black Hole Production in String Theory, *J. Cosmol. Astropart. Phys.* **07** (2018) 005, [arXiv:1803.07626](#).
- [71] Y. Tada and S. Yokoyama, Primordial black hole tower: Dark matter, earth-mass, and LIGO black holes, *Phys. Rev. D* **100**, 023537 (2019), [arXiv:1904.10298](#).
- [72] I. Musco and J. C. Miller, Primordial black hole formation in the early universe: critical behaviour and self-similarity, *Class. Quant. Grav.* **30**, 145009 (2013), [arXiv:1201.2379](#).
- [73] T. Harada, C.-M. Yoo, and K. Kohri, Threshold of primordial black hole formation, *Phys. Rev. D* **88**, 084051 (2013), [Erratum: *Phys. Rev. D* 89, 029903 (2014)], [arXiv:1309.4201](#).
- [74] A. Escrivà, C. Germani, and R. K. Sheth, Universal threshold for primordial black hole formation, *Phys. Rev. D* **101**, 044022 (2020), [arXiv:1907.13311](#).
- [75] C.-M. Yoo, T. Harada, and H. Okawa, Threshold of Primordial Black Hole Formation in Nonspherical Collapse, *Phys. Rev. D* **102**, 043526 (2020), [arXiv:2004.01042](#).
- [76] J. R. Espinosa, D. Racco, and A. Riotto, A Cosmological Signature of the SM Higgs Instability: Gravitational Waves, *J. Cosmol. Astropart. Phys.* **09** (2018) 012, [arXiv:1804.07732](#).
- [77] Y. Lu, Y. Gong, Z. Yi, and F. Zhang, Constraints on primordial curvature perturbations from primordial black hole dark matter and secondary gravitational waves, *J. Cosmol. Astropart. Phys.* **12** (2019) 031, [arXiv:1907.11896](#).
- [78] V. De Luca, G. Franciolini, and A. Riotto, NANOGrav Data Hints at Primordial Black Holes as Dark Matter, *Phys. Rev. Lett.* **126**, 041303 (2021), [arXiv:2009.08268](#).
- [79] K. Inomata, M. Kawasaki, K. Mukaida, and T. T. Yanagida, NANOGrav Results and LIGO-Virgo Primordial Black Holes in Axionlike Curvaton Models, *Phys. Rev. Lett.* **126**, 131301 (2021), [arXiv:2011.01270](#).

- [80] V. Vaskonen and H. Veermäe, Did NANOGrav see a signal from primordial black hole formation?, *Phys. Rev. Lett.* **126**, 051303 (2021), [arXiv:2009.07832](#).
- [81] K. Kohri and T. Terada, Solar-Mass Primordial Black Holes Explain NANOGrav Hint of Gravitational Waves, *Phys. Lett. B* **813**, 136040 (2021), [arXiv:2009.11853](#).
- [82] G. Domènech and S. Pi, NANOGrav Hints on Planet-Mass Primordial Black Holes, (2020), [arXiv:2010.03976](#).
- [83] S. Vagnozzi, Implications of the NANOGrav results for inflation, *Mon. Not. Roy. Astron. Soc.* **502**, L11 (2021), [arXiv:2009.13432](#).
- [84] M. Kawasaki and H. Nakatsuka, Gravitational waves from type II axion-like curvaton model and its implication for NANOGrav result, *J. Cosmol. Astropart. Phys.* **05** (2021) 023, [arXiv:2101.11244](#).
- [85] B. J. Carr, K. Kohri, Y. Sendouda, and J. Yokoyama, New cosmological constraints on primordial black holes, *Phys. Rev. D* **81**, 104019 (2010), [arXiv:0912.5297](#).
- [86] R. Laha, Primordial Black Holes as a Dark Matter Candidate Are Severely Constrained by the Galactic Center 511 keV  $\gamma$ -Ray Line, *Phys. Rev. Lett.* **123**, 251101 (2019), [arXiv:1906.09994](#).
- [87] B. Dasgupta, R. Laha, and A. Ray, Neutrino and positron constraints on spinning primordial black hole dark matter, *Phys. Rev. Lett.* **125**, 101101 (2020), [arXiv:1912.01014](#).
- [88] H. Niikura *et al.*, Microlensing constraints on primordial black holes with Subaru/HSC Andromeda observations, *Nature Astron.* **3**, 524 (2019), [arXiv:1701.02151](#).
- [89] K. Griest, A. M. Cieplak, and M. J. Lehner, New Limits on Primordial Black Hole Dark Matter from an Analysis of Kepler Source Microlensing Data, *Phys. Rev. Lett.* **111**, 181302 (2013).
- [90] P. Tisserand *et al.* (EROS-2), Limits on the Macho Content of the Galactic Halo from the EROS-2 Survey of the Magellanic Clouds, *Astron. Astrophys.* **469**, 387 (2007), [arXiv:astro-ph/0607207](#).
- [91] Y. Ali-Haïmoud and M. Kamionkowski, Cosmic microwave background limits on accreting primordial black holes, *Phys. Rev. D* **95**, 043534 (2017), [arXiv:1612.05644](#).
- [92] V. Poulin, P. D. Serpico, F. Calore, S. Clesse, and K. Kohri, CMB bounds on disk-accreting massive primordial black holes, *Phys. Rev. D* **96**, 083524 (2017), [arXiv:1707.04206](#).
- [93] C. J. Moore, R. H. Cole, and C. P. L. Berry, Gravitational-wave sensitivity curves, *Class. Quant. Grav.* **32**, 015014 (2015), [arXiv:1408.0740](#).

- [94] C. T. Byrnes, M. Gerstenlauer, S. Nurmi, G. Tasinato, and D. Wands, Scale-dependent non-Gaussianity probes inflationary physics, *J. Cosmol. Astropart. Phys.* **10** (2010) 004, [arXiv:1007.4277](#).
- [95] G. Franciolini, A. Kehagias, S. Matarrese, and A. Riotto, Primordial Black Holes from Inflation and non-Gaussianity, *J. Cosmol. Astropart. Phys.* **03** (2018) 016, [arXiv:1801.09415](#).
- [96] A. Kehagias, I. Musco, and A. Riotto, Non-Gaussian Formation of Primordial Black Holes: Effects on the Threshold, *J. Cosmol. Astropart. Phys.* **12** (2019) 029, [arXiv:1906.07135](#).
- [97] V. Atal and C. Germani, The role of non-gaussianities in Primordial Black Hole formation, *Phys. Dark Univ.* **24**, 100275 (2019), [arXiv:1811.07857](#).
- [98] F. Ricciardi, M. Taoso, and A. Urbano, Solving peak theory in the presence of local non-gaussianities, *J. Cosmol. Astropart. Phys.* **08** (2021) 060, [arXiv:2102.04084](#).
- [99] L. Verde, L.-M. Wang, A. Heavens, and M. Kamionkowski, Large scale structure, the cosmic microwave background, and primordial non-gaussianity, *Mon. Not. Roy. Astron. Soc.* **313**, L141 (2000), [arXiv:astro-ph/9906301](#).
- [100] E. Komatsu and D. N. Spergel, Acoustic signatures in the primary microwave background bispectrum, *Phys. Rev. D* **63**, 063002 (2001), [arXiv:astro-ph/0005036](#).